Ren et al. *Zool. Res.* 2024, 45(5): 1116−1130
https://doi.org/10.24272/j.issn.2095-8137.2024.046
https://cstr.cn/32248.14.zr.2024.046

ZR | Zoological Research

Article Open Access

foxl2l is a germ cell-intrinsic gatekeeper of oogenesis in zebrafish

Zhiqin Ren[1], Ding Ye[1,2,3,4,*], Naike Su[1,3], Chaofan Wang[1,4], Lijia He[1,3], Houpeng Wang[1], Mudan He[1,3], Yonghua Sun[1,2,3]

[1] *Key Laboratory of Breeding Biotechnology and Sustainable Aquaculture*, *Hubei Hongshan Laboratory*, *Institute of Hydrobiology*, *Innovation Academy for Seed Design*, *Chinese Academy of Sciences*, *Wuhan*, *Hubei* 430072, *China*

[2] *School of Marine Biology and Fisheries*, *Hainan University*, *Haikou*, *Hainan* 570228, *China*

[3] *College of Advanced Agricultural Sciences*, *University of Chinese Academy of Sciences*, *Beijing* 100049, *China*

[4] *College of Fisheries and Life Science*, *Dalian Ocean University*, *Dalian*, *Liaoning* 116023, *China*

ABSTRACT

Zebrafish serve as a valuable model organism for studying germ cell biology and reproductive processes. The AB strain of zebrafish is proposed to exhibit a polygenic sex determination system, where most males initially develop juvenile ovaries before committing to male fate. In species with chromosomal sex determination, gonadal somatic cells are recognized as key determinants of germ cell fate. Notably, the loss of germ cells in zebrafish leads to masculinization, implying that germ cells harbor an intrinsic feminization signal. However, the specific signal triggering oogenesis in zebrafish remains unclear. In the present study, we identified *foxl2l* as an oocyte progenitor-specific gene essential for initiating oogenesis in germ cells. Results showed that *foxl2l*-knockout zebrafish bypassed the juvenile ovary stage and exclusively developed into fertile males. Further analysis revealed that loss of *foxl2l* hindered the initiation of oocyte-specific meiosis and prevented entry into oogenesis, leading to premature spermatogenesis during early gonadal development. Furthermore, while mutation of the pro-male gene *dmrt1* led to fertile female differentiation, simultaneous disruption of *foxl2l* in *dmrt1* mutants completely blocked oogenesis, with a large proportion of germ cells arrested as germline stem cells, highlighting the crucial role of *foxl2l* in oogenesis. Overall, this study highlights the unique function of *foxl2l* as a germ cell-intrinsic gatekeeper of oogenesis in zebrafish.

Keywords: *foxl2l*; *dmrt1*; Oogenesis; Sex determination; Meiosis

INTRODUCTION

Gonadal differentiation refers to the process by which gonads develop from an undifferentiated state into functional testes or ovaries. In species with a single sex-determining gene, such as *SRY* in mammals and *dmy* in medaka fish (Koopman, 1999; Matsuda et al., 2002), these genes regulate a cascade of downstream genes directing gonadal differentiation (Cutting et al., 2013; Li et al., 2022; Nagahama et al., 2021). However, the AB strain of zebrafish, widely used in genetic, developmental, and medical research, exhibits a polygenic sex determination system due to chromosomal alterations during domestication (Wilson et al., 2014). Despite the interaction of multiple genes and the influence of various environmental factors (Aharon & Marlow, 2021; Anderson et al., 2012; Devlin & Nagahama, 2002), sex differentiation processes in zebrafish remain largely conserved (Lin et al., 2017; Webster et al., 2017; Yang et al., 2017). Orthologs of gonadal somatic genes involved in sex differentiation in other species perform similar roles in zebrafish. For instance, the loss of critical granulosa cell differentiation factors, *foxl2a* and *foxl2b*, results in female-to-male sex reversal (Yang et al., 2017). Additionally, the loss of enzymes involved in estrogen or androgen biosynthesis, such as *cyp11a2*, *cyp17a1* *cpy19a1a*, and *cyp11c1*, also disrupts female and male differentiation (Lau et al., 2016; Li et al., 2020; Wang et al., 2022; Zhai et al., 2018; Zhang et al., 2020b). Furthermore, dysfunction of the key transcription factor for male development, *dmrt1*, leads to a female differentiation bias and spermatogenesis arrest (Lin et al., 2017; Webster et al., 2017). Despite these insights, the mechanisms underlying gonadal differentiation in zebrafish remain incompletely understood.

Zebrafish germ cells play a vital role in sex differentiation. During embryonic development, the number of primordial

Received: 13 April 2024; Accepted: 20 May 2024; Online: 21 May 2024
Foundation items: This work was supported by the National Natural Science Foundation of China (32025037), Ministry of Science and Technology of China (2023YFD2401603), Ministry of Agriculture and Rural Affairs of China (NK2022010207), Science and Technology Special Fund of Hainan Province (ZDYF2024XDNY256), and Natural Science Foundation of Wuhan
*Corresponding author, E-mail: yeding@ihb.ac.cn

germ cells (PGCs) significantly influences zebrafish sex, with a lack or lower number of PGCs leading to masculinization and a higher number promoting feminization (Siegfried & Nüsslein-Volhard, 2008; Slanchev et al., 2005; Tzung et al., 2015; Ye et al., 2019). Recent studies have shown that the knockout of germ cell-specific factors, like *figla*, *nobox*, *gdf9*, and *bmp15*, results in defective oocyte formation and an all-male phenotype in zebrafish (Chen et al., 2022; Dranow et al., 2016; Qin et al., 2022, 2018; Zhai et al., 2023). Moreover, environmental factors such as temperature, hormone levels, fatty acid metabolism, and social interactions can affect zebrafish sex and reproduction (Abozaid et al., 2011; Dang & Kienzler, 2019; Li et al., 2024; Ribas et al., 2017; Santos et al., 2017; Xu et al., 2023). During early gonadal development, most zebrafish initially develop juvenile ovaries, but some fail to mature and instead undergo sex reversal, resulting in masculinization (Luzio et al., 2021; Uchida et al., 2002; Wang et al., 2007; Wilson et al., 2024). Although zebrafish lack a single sex-determining gene, many genes and signaling pathways involved in gonadal differentiation are conserved compared among vertebrates. As such, zebrafish can serve as an ideal model organism for studying gonadal differentiation processes.

Forkhead box (FOX) proteins are a family of transcription factors characterized by a highly conserved DNA-binding domain known as the “forkhead box” or “winged helix” domain (Jackson et al., 2010). This domain enables FOX proteins to bind to specific DNA sequences, thereby regulating the expression of target genes. The FOX protein family is diverse, with over 60 members identified in zebrafish (Zeng et al., 2020), each exhibiting distinct tissue-specific expression patterns and functions. Among these, *foxl2a* and *foxl2b*, expressed in granulosa cells, are essential for ovarian development in zebrafish, with their orthologs performing similar functions in many other organisms (Georges et al., 2014; Yang et al., 2017). Interestingly, teleost fish possess an additional *foxl2* paralog, *foxl2l* (or *foxl3*), absent in mammalian genomes. Unlike *foxl2a/b*, *foxl2l* is specifically expressed in germ cells, implying unique functions.

Researchers have identified *foxl3* as a germ cell-intrinsic sex determination factor in medaka (*Oryzias latipes*) (Nishimura et al., 2015). Loss of *foxl3* enables germ cells to undergo spermatogenesis within the ovary, challenging the traditional view that gonadal somatic cells determine germ cell fate. Studies have also demonstrated that *foxl3* inhibits spermatogenesis while promoting meiosis by activating downstream factors f-box protein 47 (*fbxo47*) and REC8 meiotic recombination protein a (*rec8a*) (Kikuchi et al., 2019, 2020). Similarly, *foxl3* is reported to play a comparable role in sex differentiation in tilapia (*Oreochromis niloticus*) (Dai et al., 2021). Both species possess dominant sex-determining genes, with *dmy* (also known as *dmrt1y*) in medaka and *amhy* in tilapia acting as primary regulators of sex differentiation (Li et al., 2015; Matsuda et al., 2002; Nanda et al., 2002). In contrast, zebrafish lack a single sex-determining gene, making the investigation of the role of *foxl3* in zebrafish particularly intriguing. Recent research has indicated that *foxl2l*, the zebrafish ortholog of *foxl3*, is specifically expressed in oocyte progenitors, suggesting a potential role in zebrafish oogenesis (Liu et al., 2022). However, the precise function of *foxl2l* remains unknown.

In this study, we established a *foxl2l*-knockout zebrafish model using CRISPR/Cas9 technology to investigate the role of *foxl2l* in oogenesis. The *foxl2l*-knockout zebrafish bypassed the juvenile ovary stage and developed into fertile males, highlighting the crucial role of *foxl2l* in sex differentiation. Further analysis revealed that loss of *foxl2l* impeded the initiation of meiosis and obstructed entry into oogenesis, resulting in premature spermatogenesis during early gonadal development. Furthermore, by creating double mutants of *foxl2l* and the pro-male gene *dmrt1*, we demonstrated that simultaneous loss of both genes led to the complete blockage of germ cell differentiation, with a significant proportion of cells arrested in an undifferentiated state. These findings highlight the indispensable role of *foxl2l* in oogenesis. This study identified the unique function of *foxl2l* as a gatekeeper of oogenesis in zebrafish gametogenesis and sex differentiation.

MATERIALS AND METHODS

Fish and maintenance

All experiments in this study were performed on AB strain zebrafish. All zebrafish were maintained and raised as described previously (Kimmel et al., 1995) at the China Zebrafish Resource Center of the National Aquatic Biological Resource Center (CZRC-NABRC, Wuhan, China, http://zfish.cn). The experiments involving zebrafish followed the Zebrafish Usage Guidelines of the China Zebrafish Resource Center (CZRC) and were performed under the approval of the Institutional Animal Care and Use Committee of the Institute of Hydrobiology, Chinese Academy of Sciences (protocol number IHB2014-006).

Establishment of mutant lines

The CRISPR/Cas9 system was applied to generate zebrafish mutant lines according to previously reported protocols (Zhang et al., 2020a). Target sites were designed using an online tool (http://www.crisprscan.org/). The single-guide RNA (sgRNA) and Cas9 mRNA were prepared using MEGAscript T7 and mMESSAGE mMACHINE T3 kits (Life Technologies, USA), respectively. A mixture of 1 nL, containing 400 ng/μL Cas9 mRNA and 50 ng/μL sgRNA, was co-injected into one-cell-stage embryos to generate the F0 mutant fish. The mutations were identified by PCR and sequencing. F0 fish carrying mutations were raised and outcrossed with wild-type (WT) fish to produce F1 offspring.

Sampling and histological analysis

Zebrafish were anesthetized by MS222 (Sigma-Aldrich, USA) and imaged with a digital camera (Canon EOS 700D, Japan). Whole fish were then fixed in Bouin's fixative for 24 h before processing. After standard histological processing, the samples were embedded in paraffin and sectioned at 2 μm using a microtome (HM340E, Thermo Scientific, USA). The sections were viewed and imaged under a microscope (Olympus BX53, Japan) or scanned with Aperio VERSA (Leica, Germany).

Single-molecule fluorescence *in situ* hybridization (sm-FISH)

For whole-mount sm-FISH, zebrafish gonads were fixed in 4% paraformaldehyde (PFA) overnight at 4°C and processed for hybridization following previously described protocols (Choi et al., 2018; Dirks & Pierce, 2004). At least five pairs of probes were designed for each gene detected. After fixation, the samples were washed with PBST three times for 5 min each, then permeabilized with 10 μg/mL proteinase K for 20 min.

The samples were then washed with saline-sodium citrate buffer (SSCT) three times for 5 min each, then incubated with the probe overnight at 37°C. After washing four times, the samples were incubated with labeled hairpins to initiate hybridization chain reaction (HCR) at room temperature for 4 h in the dark. Excess hairpins were removed by washing with SSCT, after which the samples were stained with 1 μg/mL DAPI for 30 min and mounted with VECTASHIELD® mounting medium (Vector Laboratories, USA). Confocal images were acquired using a laser-scanning confocal inverted microscope (Leica SP8, Germany) with a 63× oil-immersed objective and processed with Fiji software (Schindelin et al., 2012).

RNA sequencing (RNA-seq) and analysis

The zebrafish were sampled at 15 and 20 days post-fertilization (dpf). Three fish trunks, including the gonads, were pooled into one sample and preserved in RNA stabilizer after dissection. Total RNA was extracted and purified using a FastPure Complex Tissue/Cell Total RNA Isolation Kit (Vazyme, China). RNA quality was determined by Nanodrop, Qubit, and Labchip GX. For each sample, 50 ng of RNA was used to prepare VAHTS RNA-seq libraries using a Universal V6 RNA-seq Library Prep Kit for Illumina (Vazyme, China). Sequencing was performed on the Illumina NextSeq 500 platform (USA) with 150 bp paired-end (PE) reads at the Analysis and Testing Center of Institute of Hydrobiology, Chinese Academy of Sciences, China. Clean data were mapped to zebrafish reference transcripts generated from genome GRCz11 Ensembl release 97. Differential expression analysis was performed using DESeq2 (Love et al., 2014), with genes exhibiting an adjusted P<0.05 considered as differentially expressed genes (DEGs). DEGs were subjected to Gene Ontology (GO) enrichment analysis. GO enrichment analysis and visualization were performed using ClusterProfiler v.4.0 (Wu et al., 2021).

Quantitative PCR (qPCR)

The zebrafish were sampled at 35 dpf. Two fish trunks were pooled into one sample and maintained in RNA stabilizer after dissection. Total RNA was extracted using a FlaPure Animal Tissue Total RNA Extraction Kit (Beijing Genesand Biotech, China). cDNA was synthesized with an HiScript III All-in-One RT SuperMix Perfect for qPCR Kit (Vazyme, R333-01, China). qPCR was performed using a CFX96 Touch Real-Time PCR Detection System (BioRad, USA) and Taq Pro Universal SYBR qPCR Master Mix (Vazyme, Q712-02, China). *ef1a* was used as a reference gene as its expression was invariant in the WT and *foxl2l*$^{-/-}$ gonads. The expression levels of *foxl2l* and *dmrt1* were analyzed. The primer pairs were: *ef1a*: *ef1a*-F (5'-GGCTGACTGTGCTGTGCTGATTG-3') and *ef1a*-R (5'-CTTGTCGGTGGGACGGCTAGG-3'); *foxl2l*: *foxl2l*-F (5'-GGTCTGTAGGACGGGTGAAAATG-3') and *foxl2l*-F (5'-CAATCTGAGCCTGAACGAGTG-3'); and *dmrt1*: *dmrt1*-F (5'-CGATGATCAACGCTGAGAA-3') and *dmrt1*-R (5'-AACCTTATAGAACGACCCCT-3').

Immunofluorescence

Immunofluorescence staining was performed following previously described procedures (Ye et al., 2023). Antibodies labeled for Piwil1 and Sycp3, as well as primary antibodies for nanos2 used, were generated in a prior study (Ye et al., 2023). For whole-mount immunofluorescence staining, zebrafish gonads were fixed in 4% PFA overnight at 4°C. For section immunofluorescence staining, zebrafish gonads were fixed in 2% PFA at room temperature for 2 h, then transferred to a series of sucrose solutions with increasing concentrations (5%, 8%, 12%,16%, and 20% sucrose) for 30 min each. Samples were embedded in optimal cutting temperature (OCT) medium and sectioned at 12 μm using a CM5030 cryostat (Leica, Germany). The sections were washed three times for 5 min each with PBSBDT (2% bovine serum albumin (BSA), 1% dimethyl sulfoxide (DMSO), and 0.1% Triton X-100 in phosphate-buffered saline (PBS)), then blocked in PBSBDT for 2 h at room temperature. After blocking, the samples were incubated with primary antibodies diluted in PBSBDT overnight at 4°C, followed by incubation with anti-rabbit Alexa Fluor 488 secondary antibody (Molecular Probes, RRID: AB_2535792, USA) for 2 h at room temperature. The samples were then mounted with VECTASHIELD® mounting medium. Confocal images were acquired using a laser-scanning confocal inverted microscope (Leica SP8, Germany) with a 63× oil-immersed objective and processed with Fiji software (Schindelin et al., 2012).

Estradiol (E2) treatment

For E2 treatment, the progeny of *foxl2l*$^{+/-}$ and *foxl2l*$^{-/-}$ fish were used, with random distribution into different groups. The 15 dpf fry were exposed to 0.50 nmol/L E2 for 25 days until 40 dpf. The water was changed twice a day with freshly added E2. After the treatment period, the fish were allowed to recover for 5 days. At 45 dpf, all fish were anesthetized with MS222 and fixed for histological analysis.

Data analysis

All results are expressed as mean±standard error of the mean (SEM). Statistical significance was analyzed by one-way analysis of variance (ANOVA) (between more than two groups) or unpaired Student's *t*-test using (between two groups) Prism software (GraphPad, USA). Statistical significance was set to *: P<0.05, **: P<0.01, and ***: P<0.001.

RESULTS

***foxl2l* deficiency led to all-male development**

To elucidate the role of *foxl2l* during the critical period of zebrafish gonadal differentiation, sm-FISH was first applied to detect the expression of *foxl2l* in the gonads at the juvenile ovary stage (Figure 1A). In 30 dpf ovaries with abundant IB stage oocytes, *foxl2l* was primarily expressed in synchronously dividing germ cells within germ cell cysts, which may be mitotic oogonia or prefollicular IA stage (also known as chromatin nucleolar stage) oocytes entering meiosis (Figure 1A). Additionally, weak *foxl2l* expression was observed in IB stage oocytes (Figure 1A asterisk). In putative males, where no or very few IB stage oocytes were observed, *foxl2l* was specifically expressed in germ cells within the cysts. These findings indicate that during the juvenile ovary stage, *foxl2l* is predominantly expressed in germ cells within germ cell cysts, suggesting a potential function in germ cell differentiation.

To investigate the function of *foxl2l*, CRISPR/Cas9 was employed to target the forkhead box domain of the *foxl2l* gene. A mutant line was generated with a 13 bp deletion resulting in a frame-shift mutation (Figure 1B). Protein structure predictions using AlphaFold indicated that, compared to the WT Foxl2l protein, the mutation in the critical forkhead box domain led to misfolding, disrupting the protein structure and presumably causing functional inactivation (Figure 1C).

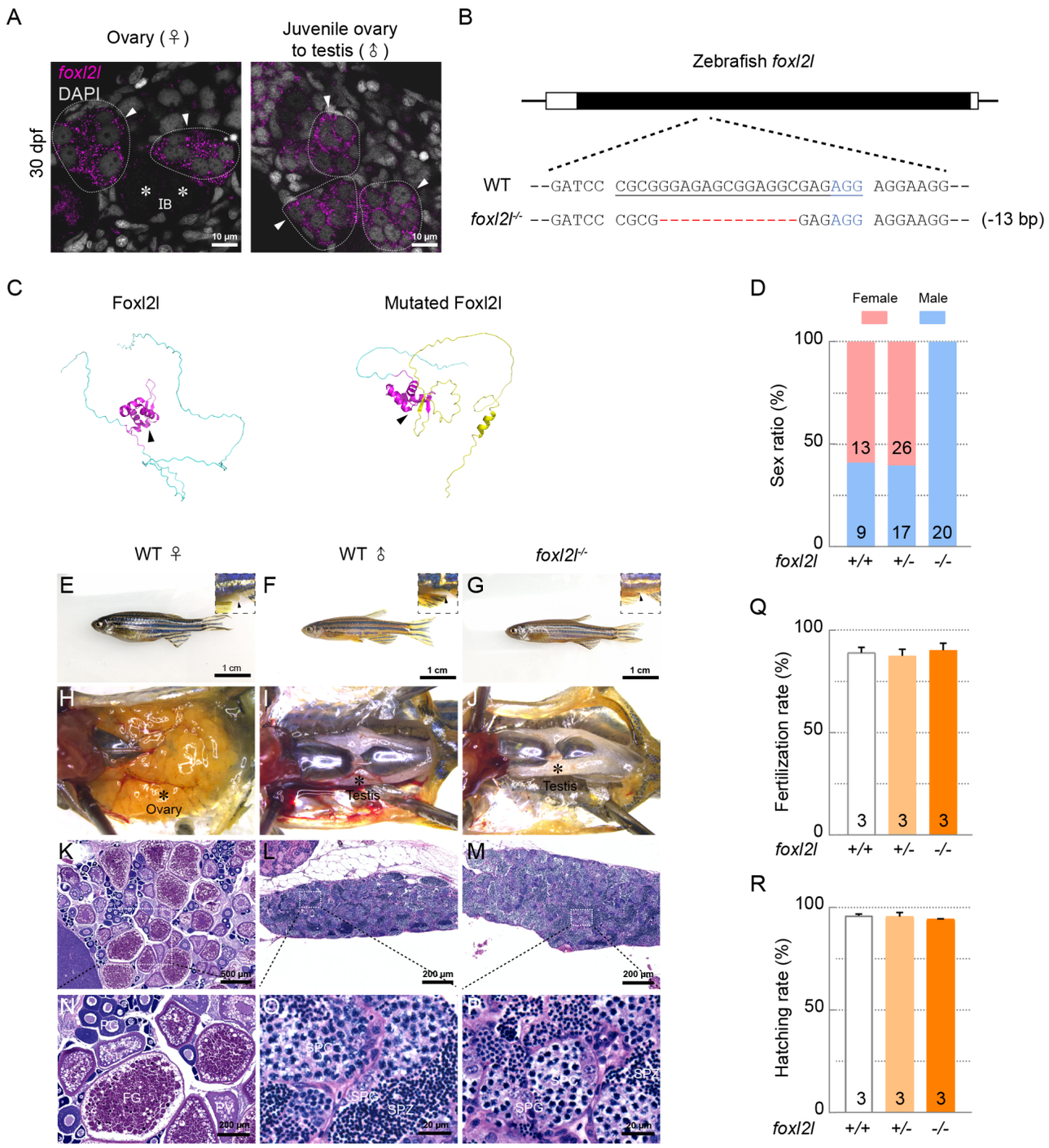

Figure 1 Loss of *foxl2l* led to an all-male phenotype in zebrafish

A: sm-FISH detection of *foxl2l* expression in zebrafish gonads during sex differentiation. In females, *foxl2l* was mainly expressed in synchronously dividing germ cells (arrowheads) within germ cell cysts (circled with white dashed lines) and weakly in IB stage oocytes (asterisks). In putative males, *foxl2l* was also expressed in germ cell cysts. Scale bars: 10 μm. B: Schematic of *foxl2l* gene structure and CRISPR/Cas9-induced mutation. Mutant line with a 13 bp deletion was generated for phenotype analysis. Underlined sequence is CRISPR site, protospacer adjacent motif (PAM) sequence is shown in blue, and altered sequence is shown in red. C: Structural prediction of mutant Foxl2l protein. Mutation led to misfolding of its forkhead domain (labeled in magenta). Arrowhead indicates mutation site. Falsely translated peptide is labeled in yellow. D: Sex ratio of adult fish in WT, *foxl2l*$^{+/-}$, and *foxl2l*$^{-/-}$ fish (n=22 WT, n=43 *foxl2l*$^{+/-}$, n=20 *foxl2l*$^{-/-}$). All *foxl2l*$^{-/-}$ fish developed into males. E–G: Morphology of WT females, WT males, and *foxl2l*$^{-/-}$ fish at 120 dpf. The *foxl2l*$^{-/-}$ fish developed into males only. Arrowheads indicate genital papilla. Scale bars: 1 cm. H–J: Gross morphology of gonads in WT females, WT males, and *foxl2l*$^{-/-}$ fish. Asterisks indicate gonads. K–P: Histological examination of gonads in WT females, WT males, and *foxl2l*$^{-/-}$ fish. PG, primary growth stage oocyte; PV, previtellogenic oocyte; FG, full-grown oocyte; SPG, spermatogonia; SPC, spermatocyte; SPZ, spermatozoa. Scale bars: 500 μm, 200 μm, and 20 μm. Q: Fertility analysis of male adult fish of different genotypes crossed with WT females (n=3 for each group, one-way ANOVA exhibited no significant difference, mean±SEM). The *foxl2l*$^{-/-}$ males exhibited comparable fertility to WT and *foxl2l*$^{+/-}$ males. R: Hatching rate of embryos produced with male adult fish of different genotypes and WT females (n=3 for each group, one-way ANOVA exhibited no significant differences, mean±SEM).

The impact of *foxl2l* deficiency on zebrafish sex differentiation was further assessed by comparing the sex ratio of adults at 120 dpf. All *foxl2l*-knockout (*foxl2l*$^{-/-}$) zebrafish developed as males, while WT (*foxl2l*$^{+/+}$) and heterozygous (*foxl2l*$^{+/-}$) siblings exhibited a sex ratio with approximately 60% females (Figure 1D). Anatomical and histological analyses revealed that the testis structure and spermatogenesis in *foxl2l*$^{-/-}$ males were comparable to those of the WT males (Figures 1E–P). Additionally, *foxl2l*$^{-/-}$ sperm could fertilize WT eggs normally (Figure 1Q), with a hatching rate comparable to that of the WT (Figure 1R). These findings suggest that *foxl2l* is essential for female development in zebrafish but is not necessary for male development.

***foxl2l* deficiency prevented juvenile ovary formation**

To investigate the role of *foxl2l* in gonadal development, the developmental trajectories of *foxl2l*$^{-/-}$ zebrafish were comprehensively compared at different stages, using *foxl2l*$^{+/-}$ zebrafish as the control because the heterozygous mutants did not differ developmentally from their WT siblings. At 15 dpf, the *foxl2l*$^{+/-}$ gonads contained pre-meiotic germ cells with distinctive nucleoli, forming germ cell cysts through synchronous division (Figure 2A1). Additionally, these gonads exhibited meiotic cells within the germ cell cysts, displaying typical features of IA stage oocytes. In contrast, the *foxl2l*$^{-/-}$ gonads only contained pre-meiotic germ cells within the cysts, lacking germ cells that had entered meiosis (Figure 2A2).

By 20 dpf, the *foxl2l*$^{+/-}$ gonads showed synchronized development of more meiotic germ cells or IA stage oocytes within the germ cell cysts, presenting an ovarian-like structure (juvenile ovary) (Figure 2B1). Conversely, the *foxl2l*$^{-/-}$ gonads displayed typical features of spermatogonia differentiation from type A to type B, with many germ cells exhibiting deep hematoxylin staining, disappearance of distinct nucleoli, reduced nuclear areas, and increased cell numbers within each germ cell cyst, indicating the presence of type B spermatogonia (Figure 2B2).

Starting from 25 dpf, the *foxl2l*$^{+/-}$ gonads exhibited two distinct developmental states, indicating phenotypic sexual differentiation. At 25 dpf, some individuals in the *foxl2l*$^{+/-}$ group developed numerous IB stage oocytes (Figure 2C1). These oocytes possessed peripherally distributed nucleoli in germinal vesicles and assembled with surrounding somatic cells to form primary growth (PG) stage follicles, indicating the initiation of normal oogenesis and the likelihood of future female development. In other individuals, most oocytes halted development at the IA stage, with anticipated apoptosis leading to arrested oogenesis (Figure 2C2). The ovarian-like gonads eventually transitioned to testes, with the individuals developing into males. However, in the *foxl2l*$^{-/-}$ gonads, neither IB stage oocytes nor ovarian-like structures were observed. Instead, early testicular characteristics persisted, revealed by the accumulation of abundant type B spermatogonia (Figure 2C3).

At 35 dpf, the *foxl2l*$^{+/-}$ females exhibited a rapid increase in the number of PG stage follicles (Figure 2D1), while the *foxl2l*$^{+/-}$ males were still undergoing transition from ovarian-like gonads to testes, with IA stage oocytes remaining (Figure 2D2). In the *foxl2l*$^{-/-}$ fish, type B spermatogonia further increased in number, and meiotic spermatocytes were observed, indicating ongoing spermatogenesis (Figure 2D3).

By 45 dpf, the *foxl2l*$^{+/-}$ female ovaries displayed continuous development, with some oocytes showing cortical alveoli, suggesting progression toward late-PG or previtellogenic (PV) stage follicles (Figure 2E1). The *foxl2l*$^{+/-}$ males completed the juvenile ovary to testes transition, initiating spermatogenesis with meiotic spermatocytes without any visible spermatozoa (Figure 2E2). In contrast, spermatogenesis in the *foxl2l*$^{-/-}$ fish was already completed, with observable spermatozoa (Figure 2E3).

In summary, the loss of *foxl2l* prevented germ cells from entering oogenesis and hindered the formation of juvenile ovaries, indicating that *foxl2l is* essential for initiating oogenesis. Moreover, in the absence of *foxl2l*, germ cells directly entered premature spermatogenesis, resulting in precocious spermatozoa production, thus demonstrating the role of *foxl2l* in inhibiting spermatogenesis.

***foxl2l* deficiency prevented female meiosis and oogenesis**

To elucidate the role of *foxl2l* in gonadal differentiation and identify potential regulatory factors, transcriptome analysis was conducted on *foxl2l*-knockout zebrafish at 15 and 20 dpf, coinciding with the onset of germ cell differentiation and juvenile ovary formation and aligning with previous observations of mutant phenotypes.

For each sample, over 6 gigabytes (GB) of FASTQ raw data were obtained (Supplementary Table S1). FASTQ reads were cleaned using Trimmomatic, with over 6 GB of clean data obtained for further analysis (Supplementary Table S2). GO enrichment analysis of DEGs revealed significant enrichment in terms related to meiosis and oocyte development (Figure 3A), as well as terms related to peptidase activity (Figure 3A). Genes with potential roles in meiosis were significantly down-regulated in *foxl2l*$^{-/-}$ fish at the sampled stages (Figure 3B). Additionally, oocyte-expressed genes showed little difference at 15 dpf but were significantly down-regulated at 20 dpf in *foxl2l*$^{-/-}$ fish (Figure 3C). These findings indicate that germ cells in *foxl2l*$^{-/-}$ fish do not establish a female germ cell identity, preventing entry into advanced meiosis and oogenesis.

Further analysis of the expression of representative genes associated with gametogenesis (*foxl2a*, *foxl2b*, *sox9a*, and *gsdf*) and steroid synthesis (*cyp11a2* and *hsd3b1*) in gonadal somatic cells revealed no significant differences between *foxl2l*$^{+/-}$ and *foxl2l*$^{-/-}$ fish (Figure 3D). This suggests that *foxl2l* knockout primarily affects gametogenesis and gonadal differentiation through germ cells rather than gonadal somatic cells.

To further clarify the roles of *foxl2l* in meiosis, immunofluorescence was employed to analyze germ cell development in *foxl2l*-knockout zebrafish. An antibody against Piwi-like RNA-mediated gene silencing 1 (Piwil1) was used to label germ cells, and an antibody against synaptonemal complex protein 3 (Sycp3), a protein involved in synaptonemal complex formation, was used to label the process of meiosis (Ye et al., 2023).

At 20 dpf, the *foxl2l*$^{+/-}$ gonads displayed clusters of Piwil1 and Sycp3 double-positive cells, with the distribution pattern of Sycp3 indicating entry into meiosis (Figure 4A1–4). In contrast, all Piwil1-positive cells in *foxl2l*$^{-/-}$ fish lacked Sycp3 signals, indicating the absence of germ cells entering meiosis (Figure 4B1–4). By 35 dpf, sex differentiation was evident in *foxl2l*$^{+/-}$ fish, with some individuals developing numerous PG stage follicles, indicating future female development (Supplementary Figure S1A1–4). In these fish, IA stage oocytes exhibited Piwil1 and Sycp3 double-positivity, while IB stage oocytes showed Sycp3 negativity due to reaching the

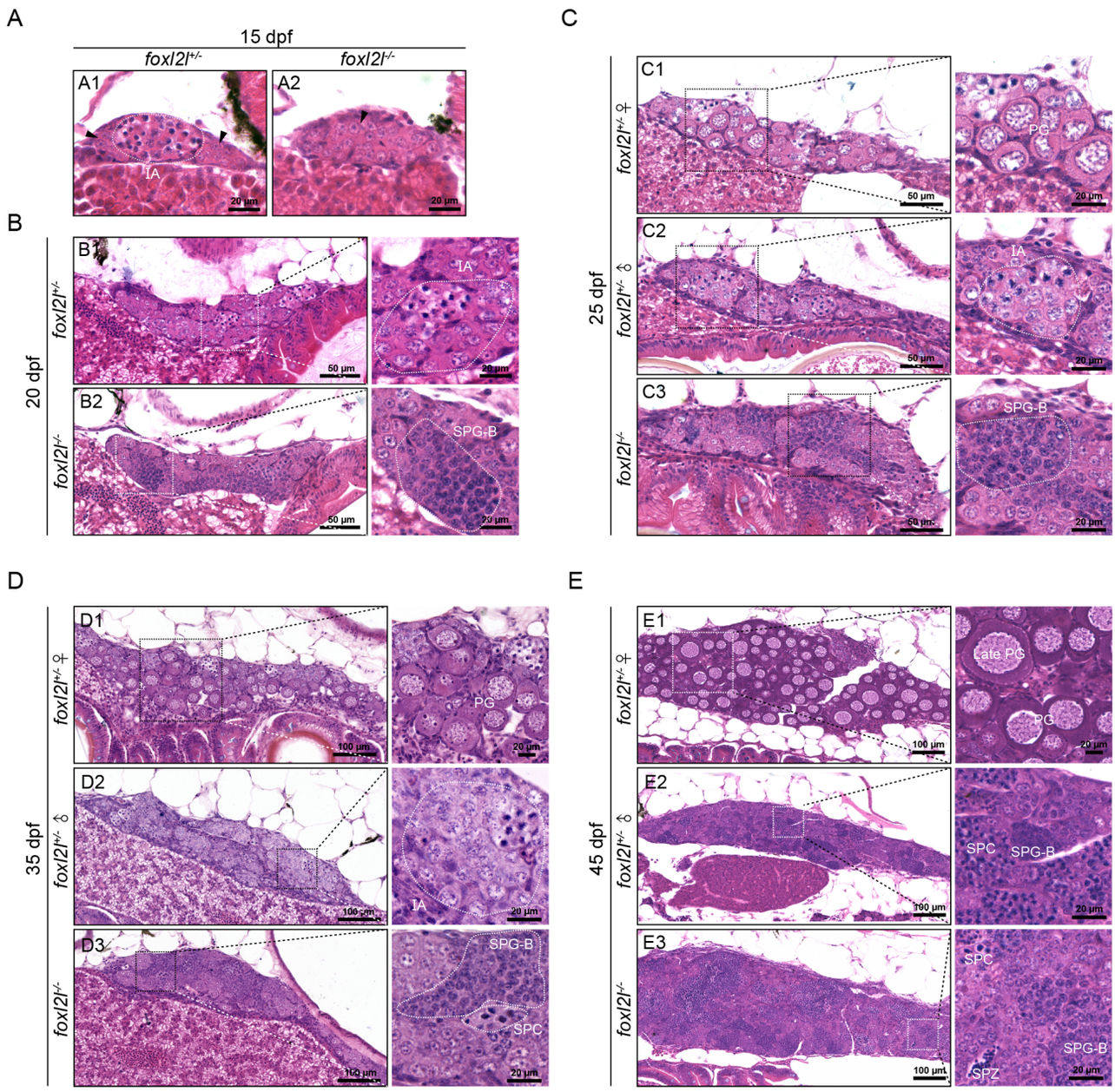

Figure 2 Histological analysis of gonads at different ages during sex differentiation and gonadal development

A1, A2: At 15 dpf, *foxl2l*$^{+/-}$ gonads contained pre-meiotic germ cells (arrowhead) and IA stage oocytes (circled with white dashed lines). The *foxl2l*$^{-/-}$ gonads only contained pre-meiotic germ cells (arrowhead). Scale bars: 20 μm. B1, B2: At 20 dpf, *foxl2l*$^{+/-}$ gonads contained more IA stage oocytes, exhibiting an ovarian-like structure. The *foxl2l*$^{-/-}$ gonads contained type B spermatogonia (SPG-B) and underwent spermatogenesis. Scale bars: 50 μm and 20 μm. C1–C3: At 25 dpf, *foxl2l*$^{+/-}$ females developed PG stage follicles in the gonads. The *foxl2l*$^{+/-}$ males only developed IA stage oocytes. The *foxl2l*$^{-/-}$ fish accumulated abundant type B spermatogonia. Scale bars: 50 μm and 20 μm. D1–D3: At 35 dpf, *foxl2l*$^{+/-}$ females exhibited increased PG stage follicles. The *foxl2l*$^{+/-}$ males transitioned from ovarian-like gonads to testis, with IA stage oocytes remaining. In *foxl2l*$^{-/-}$ fish, type B spermatogonia further increased, and meiotic spermatocytes were observed. Scale bars: 100 μm and 20 μm. E1–E3: At 45 dpf, *foxl2l*$^{+/-}$ female ovaries displayed late-PG stage follicles. The *foxl2l*$^{+/-}$ males initiated spermatogenesis with meiotic spermatocytes. In *foxl2l*$^{-/-}$ fish, spermatozoa were detected. Scale bars: 100 μm and 20 μm. IA, IA stage oocytes; PG, primary growth stage oocyte; SPG-B, type B spermatogonia; SPC, spermatocyte; SPZ, spermatozoa.

diplotene stage. Conversely, other individuals, expected to develop into males, showed persistent clusters of Piwil1 and Sycp3 double-positive cells, indicating ongoing meiosis (Figure 4C1–4). Based on these observations and previous histological analysis, these individuals were undergoing juvenile ovary to testis transition (Figure 4C1–4). Meiotic germ cells, corresponding to IA stage oocytes in the juvenile ovary, failed to progress to the diplotene stage and form IB stage oocytes. In the *foxl2l*$^{-/-}$ fish, most germ cells remained Sycp3-negative, with a few cells showing Sycp3 signals clustered at a single point, indicating preleptotene or leptotene stage germ cells. (Figure 4D1–4). At 45 dpf, the *foxl2l*$^{+/-}$ females exhibited ongoing oogenesis, with follicles increasing in size and developing into late-PG or PV stage oocytes (Supplementary Figure S1B1–4). Concurrently, the *foxl2l*$^{+/-}$ males completed juvenile ovary to testis transition, initiating spermatogenesis. The expression pattern of Sycp3 indicated that many germ cells entered primary meiosis, including spermatocytes at the

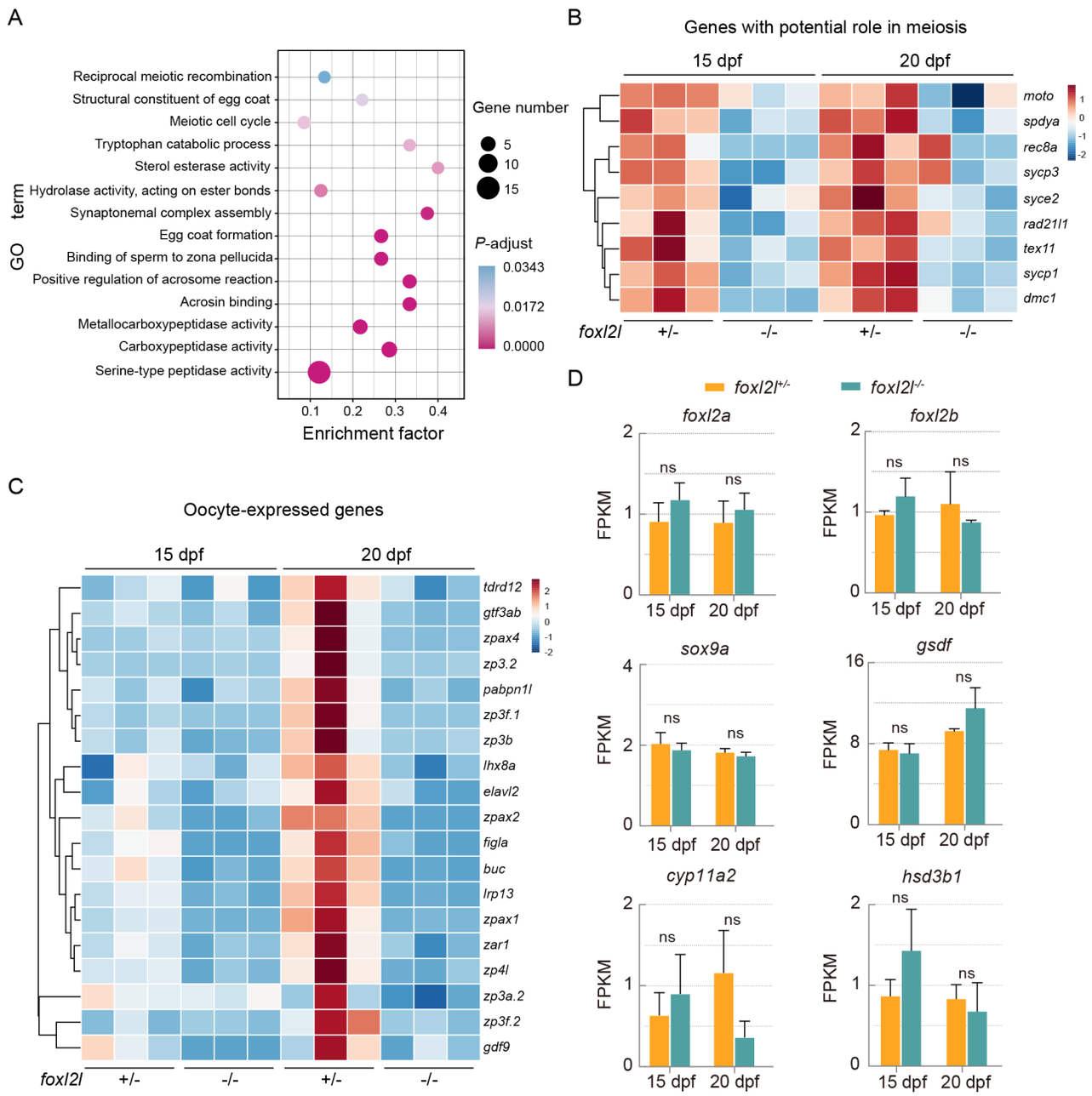

Figure 3 Transcriptomic analysis of *foxl2l*-knockout zebrafish

A: GO enrichment analysis of DEGs in *foxl2l*$^{-/-}$ and *foxl2l*$^{+/-}$ fish. B: Expression heatmap showing representative genes with potential roles in meiosis. C: Expression heatmap showing representative oocyte-expressed genes. D: Expression analysis of representative gonadal somatic cell-expressed genes (n=3 for each group, unpaired two-tailed Student's t-test, mean±SEM.; ns: Not significant). FPKM: Fragments Per Kilobase per Million.

leptotene and zygotene stages (Figure 4E1–4). However, pachytene-stage spermatocytes, spermatids, and spermatozoa were not observed (Figure 4E1–4). In the *foxl2l*$^{-/-}$ fish, spermatogenesis was complete, with visible germ cells at different meiotic stages and mature spermatozoa (Figure 4F1–4).

In summary, during the critical period of sexual differentiation, germ cells in the *foxl2l*$^{+/-}$ fish established female germ cell identity, entered advanced meiosis, and formed juvenile ovaries. In contrast, germ cells in the *foxl2l*-knockout zebrafish failed to establish female germ cell identity, instead adopting a male germ cell identity. These results highlight the essential role of *foxl2l* in maintaining female germ cell identity.

Estrogen treatment failed to rescue the phenotype of *foxl2l*-knockout zebrafish

Environmental factors can significantly impact sex differentiation in zebrafish (Dang & Kienzler, 2019; Devlin & Nagahama, 2002). Previous studies have shown that estrogen treatment can rescue oogenesis in certain mutants with an all-male phenotype, such as *cyp19a1a*, *bmp15*, and *nobox* mutants (Lau et al., 2016; Wu et al., 2023; Zhai et al., 2023). To determine whether estrogen has a similar effect on *foxl2*-knockout zebrafish, 0.50 nmol/L E2 was administered from 15 to 40 dpf for 25 days, followed by histological analysis at 45 dpf (Figure 5A) (Lau et al., 2016).

In the *foxl2l*$^{+/-}$ EtOH group, sex differentiation proceeded as expected, with PG-stage follicles observed in females and

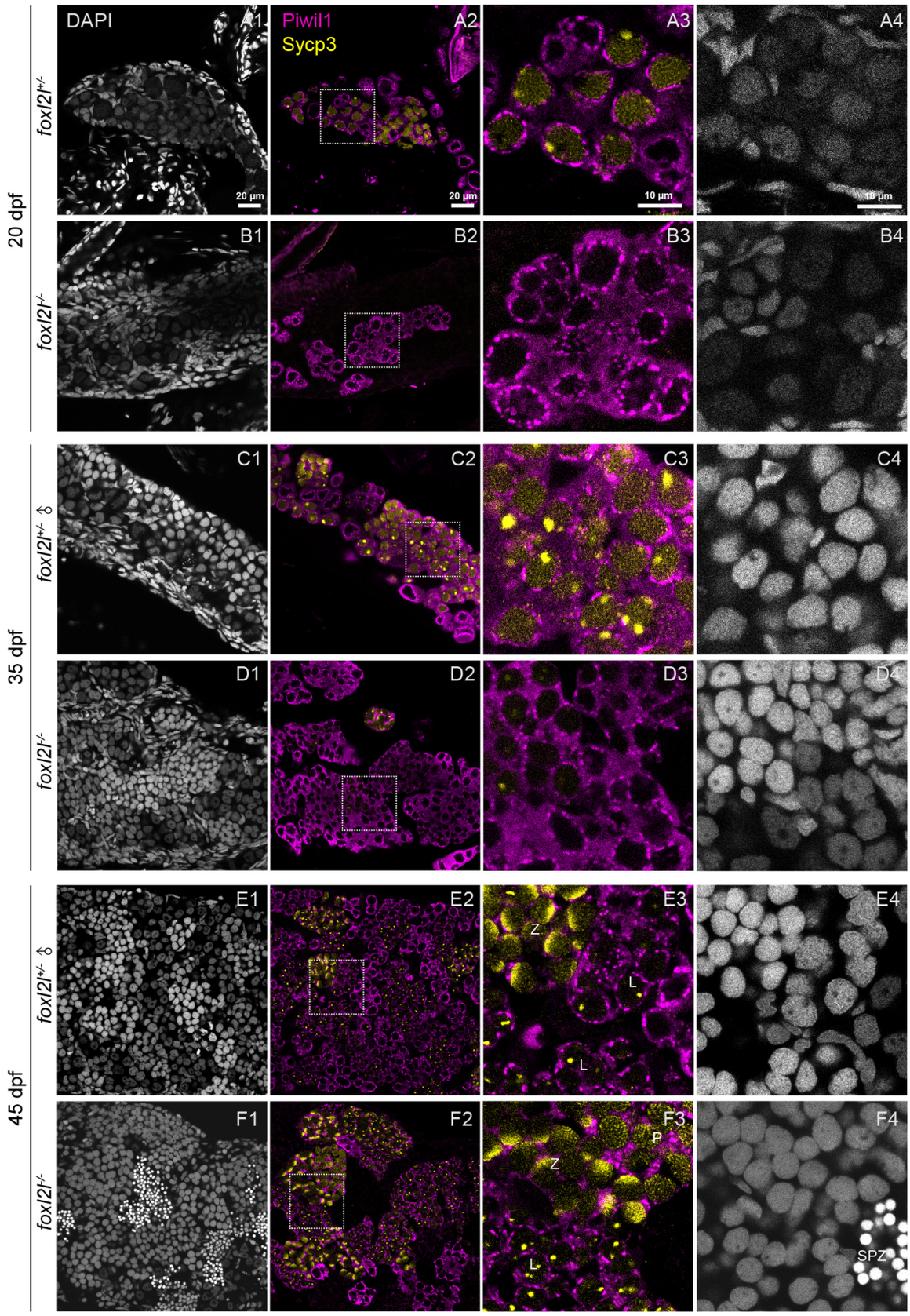

Figure 4 Meiosis progression in *foxl2l*-knockout zebrafish by co-staining of Piwil1 and Sycp3

A1–A4: At 20 dpf, *foxl2l*$^{+/-}$ fish exhibited Piwil1 (magenta) and Sycp3 (yellow) double-positive cells, with the distribution pattern of Sycp3 indicating entry into meiosis. B1–B4: At 20 dpf, *foxl2l*$^{-/-}$ fish showed no Sycp3 signal. C1–C4: At 35 dpf, *foxl2l*$^{+/-}$ males exhibited Piwil1 and Sycp3 double-positive cells. D1–D4: At 35 dpf, *foxl2l*$^{-/-}$ fish showed weak Sycp3 signals. E1–E4: At 45 dpf, *foxl2l*$^{+/-}$ males exhibited different Sycp3 expression patterns, representing leptotene (L) and zygotene stage (Z) spermatocytes. F1–F4: At 45 dpf, spermatogenesis was already completed in *foxl2l*$^{-/-}$ fish, with spermatozoa (SPZ) and spermatocytes at different meiotic stages. P, pachytene stage. Scale bars: 20 μm and 10 μm.

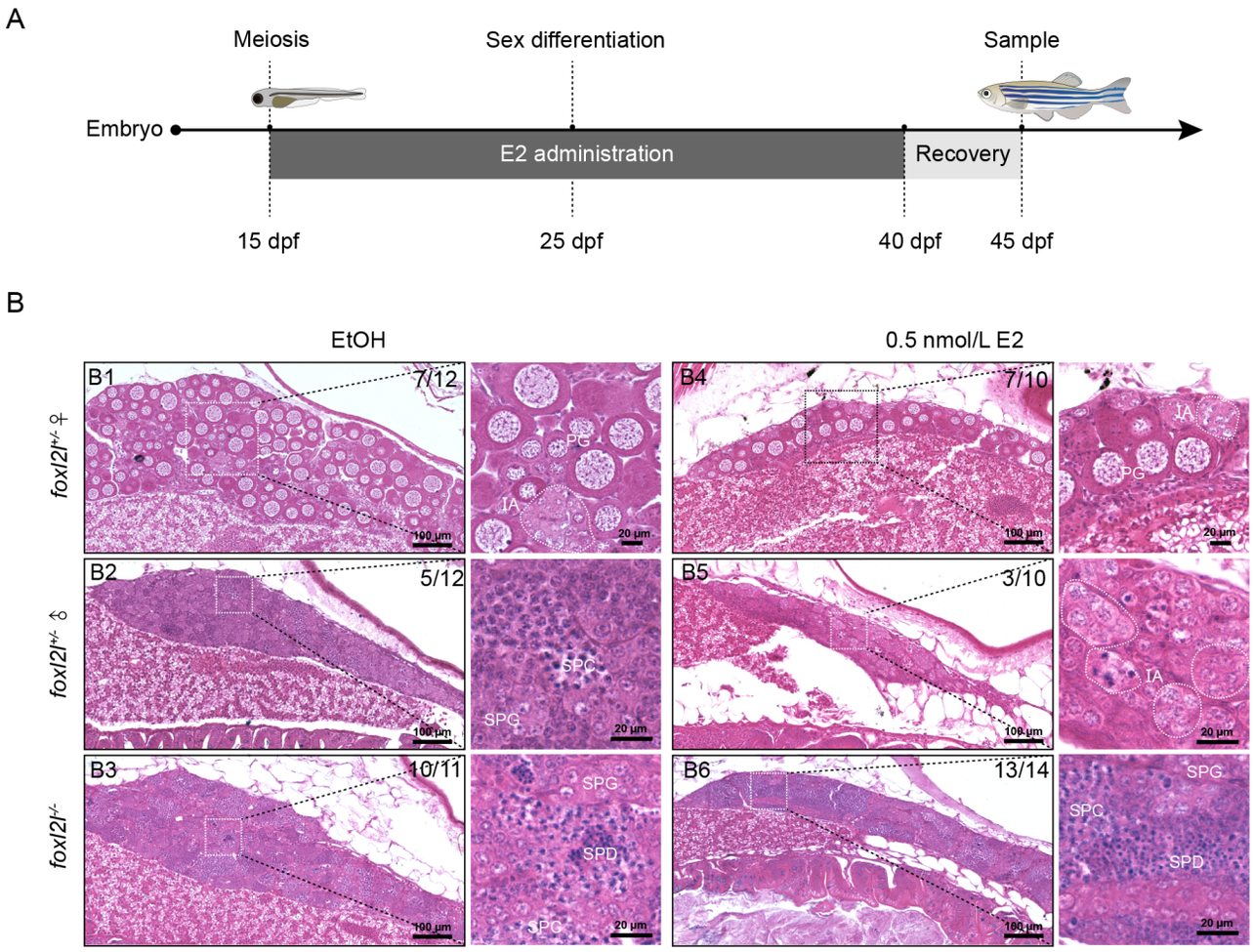

Figure 5 E2 treatment failed to rescue the phenotype of *foxl2l*-knockout zebrafish

A: Schematic of E2 treatment. B1–B6: Histological analysis of fish in different groups. Numbers represent number of fish showing representative phenotype/total number of fish in this group. IA, IA stage oocyte; PG, primary growth stage follicle; SPG, spermatogonia; SPC, spermatocyte; SPD, spermatid. Scale bars: 100 μm and 20 μm.

spermatogonia observed in males (Figure 5B1, 2). However, in the *foxl2l*$^{+/-}$ E2-treated group, gonads exhibited two distinct developmental states, with some displaying PG-stage follicles with ovarian characteristics (Figure 5B4 vs. B1), and others lacking PG-stage follicles and showing testis characteristics (Figure 5B5). These gonads differed significantly from control testes, lacking visible type B spermatogonia and primary spermatocytes, instead showing IA stage oocyte-like cells, indicating inhibition of spermatogenesis (Figure 5B5 vs. B2). These findings indicate that E2 treatment at this concentration is effective, exerting an inhibitory effect on spermatogenesis.

In the *foxl2l*$^{-/-}$ EtOH group, all individuals developed as males, with spermatocytes and spermatids present in the testes (Figure 5B3). Notably, in the *foxl2l*$^{-/-}$ E2-treated group, PG-stage follicles were not observed, indicating that E2 could not rescue oogenesis in *foxl2l*-knockout zebrafish (Figure 5B6). Furthermore, E2 failed to inhibit spermatogenesis in *foxl2l*-knockout zebrafish, as observed in the *foxl2l*$^{+/-}$ E2-treated group (Figure 5B5 vs. B6). These results suggest that the inhibitory effect of estrogen on spermatogenesis likely depends on the presence of *foxl2l*.

foxl2l was essential for oogenesis entry

The AB strain of zebrafish, with its polygenic sex determination system, displays a remarkable degree of sexual plasticity. During sex differentiation, the loss-of-function of genes promoting female development commonly results in sexual reversal from female to male (Qin et al., 2018, 2022). The all-male phenotype observed in *foxl2l*-knockout zebrafish may be due to a disruption in the balance between pro-female and pro-male gene expression during the critical period of sex differentiation. Previous studies have suggested that the *foxl2l* homolog regulates the pro-male gene *dmrt1* in Nile tilapia (Dai et al., 2021).

To determine whether *foxl2l* exerts similar functions in zebrafish, sm-FISH was employed to examine the dynamic expression patterns of *foxl2l* and *dmrt1* (Figure 6A). It is important to note that sm-FISH detects mRNA, and although *foxl2l* signals may be present in mutants, they cannot be translated into functional proteins. At 20 dpf, *foxl2l* was predominantly expressed in germ cells within germ cell cysts in *foxl2l*$^{+/-}$ fish, likely representing mitotic germ cells or IA stage oocytes (Figure 6A1). While these cells showed strongly positive *foxl2l* signals, *dmrt1* signals were remarkably low. Conversely, in *foxl2l*$^{-/-}$ fish, while *foxl2l* signals were detected in germ cells within the germ cell cyst, *dmrt1* signals were significantly higher compared to *foxl2l*$^{+/-}$ fish at the same stage (Figure 6A2). These findings suggest a potential inhibitory role of *foxl2l* on *dmrt1* expression.

At 35 dpf, sexual differentiation became evident in the

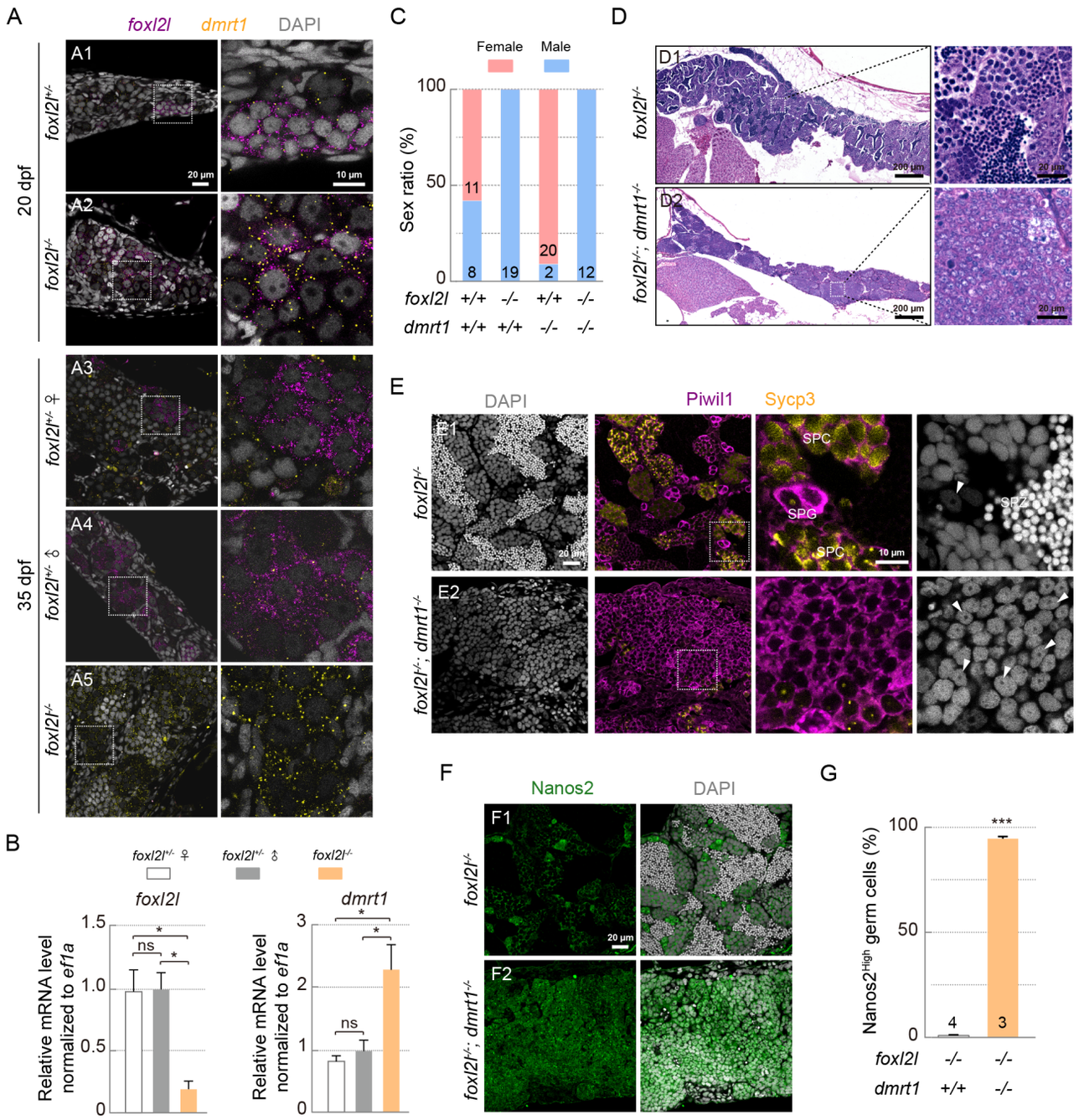

Figure 6 ***foxl2l*** **was essential for oogenesis entry**

A: sm-FISH detection of *foxl2l* (magenta) and *dmrt1* (yellow) expression in *foxl2l*-knockout zebrafish. A1: At 20 dpf, *foxl2l* was mainly expressed in germ cells within germ cell cysts in $foxl2l^{+/-}$ fish, while *dmrt1* expression was very weak in these cells. A2: At 20 dpf, *foxl2l* was expressed in cystic germ cells in $foxl2l^{-/-}$ fish, while *dmrt1* expression was significantly higher compared to $foxl2l^{+/-}$ fish. A3: At 35 dpf, $foxl2l^{+/-}$ females developed some PG stage follicles, with *foxl2l* mainly expressed in cystic germ cells and *dmrt1* showing very weak expression. A4: At 35 dpf, no PG stage follicles could be detected in $foxl2l^{+/-}$ males, with *foxl2l* mainly expressed in cystic germ cells and *dmrt1* showing very weak expression. A5: At 35 dpf, no *foxl2l* expression was detected in $foxl2l^{-/-}$ gonads, but robust *dmrt1* signals appeared. Scale bars: 20 μm and 10 μm. B: qPCR analysis of *foxl2l* and *dmrt1* mRNA expression in *foxl2l*-knockout zebrafish at 35 dpf. (n=3 for each group, one-way ANOVA, mean±SEM.; *: P<0.05; ns: Not significant). C: Sex ratio of adult fish in different genotypes (n=19 WT, n=22 $dmrt1^{-/-}$, n=19 $foxl2l^{-/-}$, n=12 $foxl2l^{-/-}$; $dmrt1^{-/-}$). *dmrt1* knockout did not rescue the all-male phenotype in *foxl2l*-knockout zebrafish. D: Histological analysis of $foxl2l^{-/-}$ and $foxl2l^{-/-}$; $dmrt1^{-/-}$ adult fish. The $foxl2l^{-/-}$ fish developed as normal males, while the $foxl2l^{-/-}$; $dmrt1^{-/-}$ fish exhibited impaired gonadal development and undifferentiated germ cells. Scale bars: 200 μm and 20 μm. E: Immunostaining of Piwil1 and Sycp3 in $foxl2l^{-/-}$ and $foxl2l^{-/-}$; $dmrt1^{-/-}$ fish. The $foxl2l^{-/-}$; $dmrt1^{-/-}$ fish contained numerous strong Piwil1-positive cells with clear nucleoli (arrowhead) and few cells with Sycp3 signals. SPG, spermatogonia; SPC, spermatocyte; SPZ, spermatozoa. Scale bars: 20 μm and 10 μm. F: Immunostaining of Nanos2 in $foxl2l^{-/-}$ and $foxl2l^{-/-}$; $dmrt1^{-/-}$ fish. Most germ cells in $foxl2l^{-/-}$; $dmrt1^{-/-}$ fish exhibited high Nanos2 expression. Scale bars: 20 μm and 10 μm. G: Statistical analysis of $Nanos2^{High}$ germ cell ratio in $foxl2l^{-/-}$ and $foxl2l^{-/-}$; $dmrt1^{-/-}$ fish. (n=4 $foxl2l^{-/-}$ fish and n=3 $foxl2l^{-/-}$; $dmrt1^{-/-}$ fish, ***: P<0.001 by unpaired two-tailed Student's t-test, mean±SEM).

foxl2l$^{+/-}$ group. In the *foxl2l*$^{+/-}$ females, *foxl2l* was predominantly expressed in germ cells within the germ cell cysts (Figure 6A3). In the *foxl2l*$^{+/-}$ males, however, their gonads were at the juvenile ovary stage, hindering oogenesis and preventing the formation of IB stage oocytes (Figure 6A4). Despite this developmental arrest, *foxl2l* expression persisted in cystic germ cells (Figure 6A4). In both the *foxl2l*$^{+/-}$ female and male gonads, *dmrt1* signals were faint in cells with strong *foxl2l* expression (Figure 6A3, 4). In contrast, *foxl2l*$^{-/-}$ fish at 35 dpf showed almost no *foxl2l* signals, which were replaced by robust *dmrt1* expression in the gonads (Figure 6A5). This suggests that loss of *foxl2l* leads to up-regulation of the pro-male gene *dmrt1* at this stage. Additionally, qPCR analysis was performed to measure the overall expression of *foxl2l* and *dmrt1* in *foxl2l*$^{+/-}$ and *foxl2l*$^{-/-}$ fish at 35 dpf. Results revealed significantly lower *foxl2l* expression in *foxl2l*$^{-/-}$ fish compared to both *foxl2l*$^{+/-}$ males and females (Figure 6B). Conversely, *foxl2l*$^{-/-}$ fish exhibited significantly higher *dmrt1* expression compared to both *foxl2l*$^{+/-}$ males and females (Figure 6B), further corroborating the sm-FISH results. In summary, these findings indicate that the up-regulation of *dmrt1* in *foxl2l*$^{-/-}$ fish results in premature spermatogenesis and an all-male phenotype.

To further explore the role of *dmrt1* in *foxl2l*-knockout zebrafish, *dmrt1*-knockout zebrafish were established with a 23 bp insertion using CRISPR/Cas9, then crossed with *foxl2l*-knockout zebrafish to obtain *foxl2l*$^{-/-}$*; dmrt1*$^{-/-}$ double mutants (Supplementary Figure S2). The sex ratio of adult fish was analyzed, revealing that while the WT sex ratio was normal, all *foxl2l*$^{-/-}$ fish developed as males (Figure 6C). Most *dmrt1*$^{-/-}$ fish developed as females, consistent with previous reports (Lin et al., 2017; Webster et al., 2017). Interestingly, *foxl2l*$^{-/-}$*; dmrt1*$^{-/-}$ fish all developed as males, indicating that *dmrt1* knockout cannot rescue the all-male phenotype observed in *foxl2l*-knockout zebrafish.

Histological analysis was conducted on the gonads of *foxl2l*$^{-/-}$*; dmrt1*$^{-/-}$ fish (Figure 6C). While the testes of *foxl2l*$^{-/-}$ fish showed normal structure and regular spermatogenesis (Figure 6D1), *foxl2l*$^{-/-}$*; dmrt1*$^{-/-}$ fish exhibited severe developmental impairment of their gonads, despite their male appearance (Figure 6D2). These gonads contained numerous undifferentiated germ cells and only a few meiotic cells. Immunofluorescence analysis was performed to detect the expression patterns of Piwil1 and Sycp3 in *foxl2l*$^{-/-}$*; dmrt1*$^{-/-}$ fish (Figure 6E). Compared to *foxl2l*$^{-/-}$ fish (Figure 6E1), *foxl2l*$^{-/-}$*; dmrt1*$^{-/-}$ fish contained many Piwil1-positive cells with one or two large clear nucleoli, characteristic of germline stem cells (Figure 6E2). Only a small number of these cells showed single-dot Sycp3 signals, indicating the absence of synaptonemal complex formation and suggesting that the cells were in the pre-meiotic stage. Immunofluorescence was also applied to detect the expression of the germline stem cell marker Nanos homolog 2 (Nanos2) in *foxl2l*$^{-/-}$*; dmrt1*$^{-/-}$ fish (Figure 6F). In *foxl2l*$^{-/-}$ fish, only a small proportion (1.193%±0.219%) of germ cells were strongly positive for Nanos2 (Figure 6F1), while the majority (95.080%±1.793%) of germ cells in *foxl2l*$^{-/-}$*; dmrt1*$^{-/-}$ fish exhibited high Nanos2 expression (Figure 6F2, G). These results indicate that the simultaneous loss of both *foxl2l* and *dmrt1* prevents normal germ cell differentiation, completely blocking both oogenesis and spermatogenesis. Consequently, germ cells in the double mutants remain in an undifferentiated state.

Premature spermatogenesis in *foxl2l*-knockout zebrafish was dependent on *dmrt1*

As described earlier, oogenesis was not restored and spermatogenesis was arrested in the *foxl2l*$^{-/-}$*; dmrt1*$^{-/-}$ adult fish. However, premature spermatogenesis was observed in *foxl2l*$^{-/-}$ fish during the early stages of gonadal differentiation. To determine whether *dmrt1* plays a role in this process, the gonadal development of *foxl2l*$^{-/-}$*; dmrt1*$^{-/-}$ fish was monitored.

At 35 dpf, the *foxl2l*$^{-/-}$ fish had initiated spermatogenesis, as evidenced by the presence of spermatocytes (Figure 7A1). In contrast, the gonads of both *foxl2l*$^{-/-}$*; dmrt1*$^{+/-}$ and *foxl2l*$^{-/-}$*; dmrt1*$^{-/-}$ fish remained undifferentiated and contained many germline stem cells (Figure 7A2, 3). This indicates that *dmrt1* is essential for the premature spermatogenesis observed in *foxl2l*$^{-/-}$ fish.

By 45 dpf, the *foxl2l*$^{-/-}$ fish had completed spermatogenesis, as evidenced by the presence of visible spermatozoa (Figure 7B1). In the *foxl2l*$^{-/-}$*; dmrt1*$^{+/-}$ fish, spermatogenesis had occurred, with spermatocytes detected, indicating that the loss of one *dmrt1* allele delayed the process of spermatogenesis in *foxl2l*$^{-/-}$ fish (Figure 7B2). However, in the *foxl2l*$^{-/-}$*; dmrt1*$^{-/-}$ fish, the gonads remained undifferentiated and filled with germline stem cells, with only a few cells showing meiotic features, indicating severe spermatogenic impairment (Figure 7B3).

At 120 dpf, the testes of *foxl2l*$^{-/-}$*; dmrt1*$^{+/-}$ fish had reached the same developmental stage as those of the *foxl2l*$^{-/-}$ fish, exhibiting similar testicular structures (Supplementary Figure S3). However, the gonadal development in the *foxl2l*$^{-/-}$*; dmrt1*$^{-/-}$ fish remained arrested at an undifferentiated state. These findings indicate that premature spermatogenesis in *foxl2l*$^{-/-}$ fish is *dmrt1*-dependent, and that *dmrt1* regulates testicular development in a dosage-dependent manner.

DISCUSSION

Zebrafish have been extensively employed in the study of germ cell biology and reproduction (Li & Ge, 2020; Wang et al., 2023; Zhu & Ge, 2018). Zebrafish are considered juvenile hermaphrodites, with most individuals initially forming ovarian-like gonads, progressing through the juvenile ovary stage, and eventually developing into functional ovaries or testes (Luzio et al., 2021; Wang et al., 2007; Wilson et al., 2024). During the juvenile ovary stage, germ cells undergo mitosis to form germ cell cysts, which then proceed to meiosis to become IA stage oocytes. In some individuals, IA stage oocytes develop into IB stage oocytes after cyst breakdown, assembling into PG stage follicles and eventually developing into females. Conversely, in other individuals, IA stage oocytes undergo apoptosis, allowing the development of spermatogenic cells and leading to male differentiation. This stage is considered the onset of sex determination and differentiation in zebrafish. However, the mechanisms regulating juvenile ovary formation in zebrafish remain largely unknown. In this study, reverse genetic approaches were employed to investigate the critical role of *foxl2l* in zebrafish gametogenesis and gonadal differentiation, with results showing that *foxl2l* acts as a germ cell-specific gatekeeper for normal oogenesis (Figure 7C).

All *foxl2l*-knockout zebrafish developed into fertile males, underscoring the importance of *foxl2l* in female development. Subsequent analysis indicated that these zebrafish did not form ovarian-like structures during gonadal development and instead underwent premature spermatogenesis. Previous

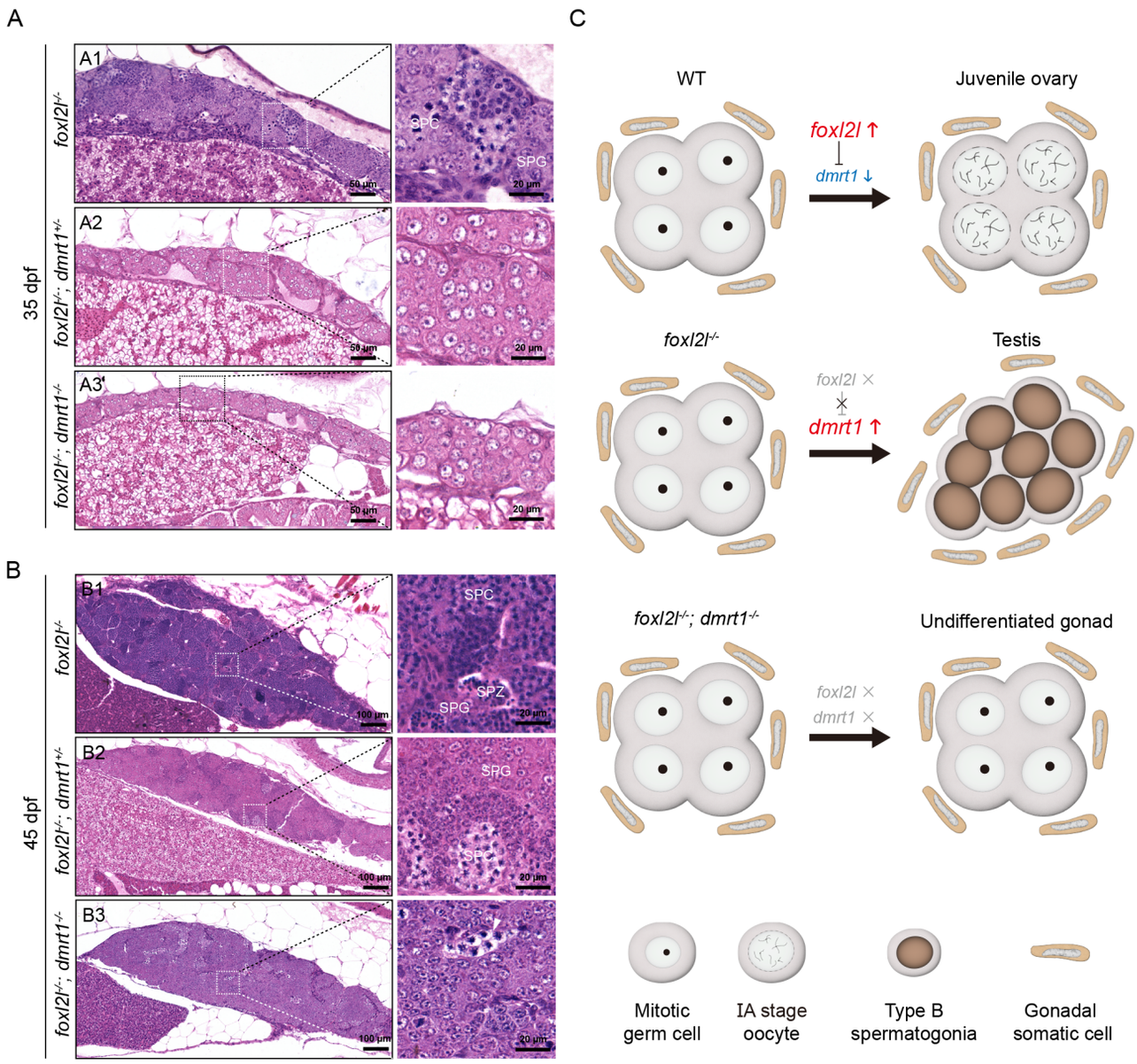

Figure 7 Knockout of *dmrt1* prevented premature spermatogenesis in *foxl2l*-knockout zebrafish

Histological analysis of gonads at 35 dpf. A1: *foxl2l*$^{-/-}$ gonads contained spermatogonia (SPG) and spermatocytes (SPC). A2, A3: Both *foxl2l*$^{-/-}$; *dmrt1*$^{+/-}$ and *foxl2l*$^{-/-}$; *dmrt1*$^{-/-}$ gonads remained undifferentiated, filled with germline stem cells. Scale bars: 50 μm and 20 μm. Histological analysis of gonads at 45 dpf. B1: *foxl2l*$^{-/-}$ fish had completed spermatogenesis, producing spermatozoa (SPZ). B2: *foxl2l*$^{-/-}$; *dmrt1*$^{+/-}$ gonads contained spermatocytes. B3: *foxl2l*$^{-/-}$; *dmrt1*$^{-/-}$ gonads were filled with germline stem cells, with a few cells exhibiting meiotic features (arrowhead). Scale bars: 100 μm and 20 μm. C: Schematic of the study.

studies have reported that the germ cell-specific transcription factors *figla* and *nobox* are crucial for zebrafish sex differentiation, with their loss resulting in an all-male phenotype (Qin et al., 2018, 2022). While mutants of these genes ultimately develop as males, their gonads still pass through the juvenile ovary stage. During early gonadal development, germ cells of these mutants differentiate into stage IA oocytes before encountering obstacles in oogenesis, which then leads to masculinization and the initiation of spermatogenesis. In contrast, *foxl2l*-knockout zebrafish did not form ovarian-like structures or differentiate into IA stage oocytes, but rather differentiated directly into type B spermatogonia, initiating spermatogenesis (Figure 7C). These findings demonstrate that *foxl2l* is crucial for the formation of juvenile ovaries in zebrafish, and its dysfunction disrupts primary female differentiation.

Early entry into meiosis is a hallmark of female germ cell development, as reported in WT Nadia zebrafish (Pan et al., 2022). In the current study, we found that *foxl2l*$^{+/-}$ gonads developed juvenile ovaries and exhibited meiotic cells at 20 dpf, whereas *foxl2l*$^{-/-}$ gonads lacked meiotic cells at the same stage. This contrasts with findings in medaka, where knockout of the *foxl2l* homolog, *foxl3*, produces differing meiotic phenotypes in genetic females and males (Nishimura et al., 2015). Notably, in genetic females, some *foxl3*-knockout germ cells switch to a spermatogenic fate and enter meiosis alongside oogenic cells, while in genetic males, *foxl3*-knockout spermatogenic cells do not undergo meiosis at the same developmental stage (Nishimura et al., 2015). Previous studies have indicated that germ cell meiosis is regulated by testicular somatic cells through paracrine signaling pathways, such as those involving retinoic acid (RA) (Crespo et al., 2019;

Griswold et al., 2012; Rodríguez-Marí et al., 2013). In medaka, the expression of sex-determining genes in gonadal somatic cells predetermines the fate of these cells during sex differentiation. However, in *foxl2l*$^{-/-}$ fish, gonadal somatic cell-expressed genes showed no significant differences compared to *foxl2l*$^{+/-}$ fish, suggesting that the germ cells in both genotypes were exposed to a similar gonadal microenvironment. This observation implies that meiosis entry in spermatogenesis and oogenesis in zebrafish is regulated by different factors, with *foxl2l* being necessary for the initiation of meiosis in oogenesis. Further in-depth research is required to elucidate the mechanisms underlying this biological phenomenon.

Given the observation of premature spermatogenesis in *foxl2l*-knockout zebrafish, the role of *foxl2l* in inhibiting spermatogenesis was further investigated. The activation of *dmrt1* in *foxl2l*$^{-/-}$ fish prompted the generation of *foxl2l*$^{-/-}$*; dmrt1*$^{-/-}$ double mutants. In both *foxl2l*$^{-/-}$*; dmrt1*$^{+/-}$ and *foxl2l*$^{-/-}$*; dmrt1*$^{-/-}$ fish, premature spermatogenesis was absent, indicating that this process in *foxl2l*-knockout zebrafish is dependent on *dmrt1* function. Therefore, *foxl2l* may inhibit spermatogenesis by suppressing *dmrt1*.

In medaka, *foxl3* knockout does not result in complete female-to-male sex reversal. XX *foxl3*-knockout medaka can simultaneously undergo spermatogenesis and oogenesis within the ovary, producing functional sperm and eggs (Nishimura et al., 2015). This indicates that while *foxl3* is not essential for sex differentiation and oogenesis in medaka, its loss disrupts oogenesis to some extent, which can be compensated through alternative pathways to produce functional eggs. In tilapia, the loss of *foxl3* results in complete female-to-male sex reversal, but in *foxl3*$^{-/-}$*; dmrt1*$^{-/-}$ tilapia, oogenesis can be partially restored, suggesting the existence of a *foxl3*-independent mechanism for oogenesis (Dai et al., 2021). In our study, *foxl2l*-knock zebrafish were unable to initiate oogenesis, and this process could not be restored in *foxl2l*$^{-/-}$*; dmrt1*$^{-/-}$ zebrafish. Instead, germ cells in these double mutants remained in a germ line stem cell state, indicating that the absence of both *foxl2l* and *dmrt1* prevents germ cell differentiation, thereby inhibiting both spermatogenesis and oogenesis (Figure 7C). These findings strongly imply that *foxl2l* serves as a critical gatekeeper of oogenesis in zebrafish.

Understanding the essential role of *foxl2l* in oogenesis and sex differentiation provides valuable insights for advancing surrogate broodstock technology in aquaculture. This technology, which involves producing donor-derived gametes from intraspecific or interspecific surrogate broodstock, is recognized as one of the most promising precision breeding methods in the field (Gui et al., 2022; Jin et al., 2021). Our recent work demonstrated the successful production of edited sperm from *Gobiocypris rarus* in zebrafish recipients using optimized spermatogonial stem cell (SSC) transplantation (Zhang et al., 2022). Despite these advances, challenges remain in producing female fish and mature eggs via SSC transplantation. Our findings on the role of *foxl2l* in oogenesis suggest that the up-regulation of *dmrt1* in the testes inhibits *foxl2l* expression, thereby preventing SSCs from entering oogenesis. Future research will focus on inducing feminization by overexpressing *foxl2l* in SSCs and transplanting these cells into PGC-depleted recipients to determine whether female fish and functional eggs can be obtained, potentially providing a theoretical basis for improving surrogate broodstock technology in aquaculture.

DATA AVAILABILITY

The raw RNA-seq data reported in this paper have been deposited in the NationalCenterforBiotechnologyInformation(NCBISRA;https://www.ncbi.nlm.nih.gov/sra/PRJNA1119569), Genome Sequence Archive (GSA: CRA016835; https://ngdc.cncb.ac.cn/gsa), and Science Data Bank (ScienceDB; DOI:10.57760/sciencedb.j00139.00059).

SUPPLEMENTARY DATA

Supplementary data to this article can be found online.

COMPETING INTERESTS

The authors declare that they have no competing interests.

AUTHORS' CONTRIBUTIONS

Z.R., D.Y., and Y.S. conceived and designed the study. Z.R., D.Y., N.S., C.W., L.H., H.W., and M.H. conducted the surveys. Z.R., D.Y., and N.S. prepared the data. Z.R. and D.Y. analyzed the data. Z.R., D.Y., and Y.S wrote the paper. All authors read and approved the final version of the manuscript.

ACKNOWLEDGMENTS

We thank Kuoyu Li from CZRC for fish care. We thank Zhixian Qiao and Xiaocui Chai from the Analysis and Testing Center of the Institute of Hydrobiology for technical support with high-throughput sequencing. We thank Fang Zhou and Guangxin Wang from the Analysis and Testing Center of the Institute of Hydrobiology for technical support with confocal microscopy.

REFERENCES

Abozaid H, Wessels S, Hörstgen-Schwark G. 2011. Effect of rearing temperatures during embryonic development on the phenotypic sex in zebrafish (*Danio rerio*). *Sexual Development*, **5**(5): 259–265.

Aharon D, Marlow FL. 2021. Sexual determination in zebrafish. *Cellular and Molecular Life Sciences*, **79**(1): 8.

Anderson JL, Marí AR, Braasch I, et al. 2012. Multiple sex-associated regions and a putative sex chromosome in zebrafish revealed by RAD mapping and population genomics. *PLoS One*, **7**(7): e40701.

Chen WT, Zhai Y, Zhu B, et al. 2022. Loss of growth differentiation factor 9 causes an arrest of early folliculogenesis in zebrafish-A novel insight into its action mechanism. *PLoS Genetics*, **18**(12): e1010318.

Choi HMT, Schwarzkopf M, Fornace ME, et al. 2018. Third-generation *in situ* hybridization chain reaction: multiplexed, quantitative, sensitive, versatile, robust. *Development*, **145**(12): dev165753.

Crespo D, Assis LHC, Van De Kant HJG, et al. 2019. Endocrine and local signaling interact to regulate spermatogenesis in zebrafish: follicle-stimulating hormone, retinoic acid and androgens. *Development*, **146**(21): dev178665.

Cutting A, Chue J, Smith CA. 2013. Just how conserved is vertebrate sex determination?. *Developmental Dynamics*, **242**(4): 380–387.

Dai SF, Qi SS, Wei XY, et al. 2021. Germline sexual fate is determined by the antagonistic action of *dmrt1* and *foxl3/foxl2* in tilapia. *Development*, **148**(8): dev199380.

Dang ZC, Kienzler A. 2019. Changes in fish sex ratio as a basis for regulating endocrine disruptors. *Environment International*, **130**: 104928.

Devlin RH, Nagahama Y. 2002. Sex determination and sex differentiation in fish: an overview of genetic, physiological, and environmental influences. *Aquaculture*, **208**(3-4): 191–364.

Dirks RM, Pierce NA. 2004. Triggered amplification by hybridization chain reaction. *Proceedings of the National Academy of Sciences of the United States of America*, **101**(43): 15275–15278.

Dranow DB, Hu K, Bird AM, et al. 2016. Bmp15 is an oocyte-produced signal required for maintenance of the adult female sexual phenotype in

zebrafish. *PLoS Genetics*, **12**(9): e1006323.

Georges A, Auguste A, Bessière L, et al. 2014. Foxl2: a central transcription factor of the ovary. *Journal of Molecular Endocrinology*, **52**(1): R17–R33.

Griswold MD, Hogarth CA, Bowles J, et al. 2012. Initiating meiosis: the case for retinoic acid. *Biology of Reproduction*, **86**(2): 35.

Gui JF, Zhou L, Li XY. 2022. Rethinking fish biology and biotechnologies in the challenge era for burgeoning genome resources and strengthening food security. *Water Biology and Security*, **1**(1): 100002.

Jackson BC, Carpenter C, Nebert DW, et al. 2010. Update of human and mouse forkhead box (*FOX*) gene families. *Human Genomics*, **4**(5): 345–352.

Jin YH, Robledo D, Hickey JM, et al. 2021. Surrogate broodstock to enhance biotechnology research and applications in aquaculture. *Biotechnology Advances*, **49**: 107756.

Kikuchi M, Nishimura T, Ishishita S, et al. 2020. *foxl3*, a sexual switch in germ cells, initiates two independent molecular pathways for commitment to oogenesis in medaka. *Proceedings of the National Academy of Sciences of the United States of America*, **117**(22): 12174–12181.

Kikuchi M, Nishimura T, Saito D, et al. 2019. Novel components of germline sex determination acting downstream of *foxl3* in medaka. *Developmental Biology*, **445**(1): 80–89.

Kimmel CB, Ballard WW, Kimmel SR, et al. 1995. Stages of embryonic development of the zebrafish. *Developmental Dynamics*, **203**(3): 253–310.

Koopman P. 1999. Sry and Sox9: mammalian testis-determining genes. *Cellular and Molecular Life Sciences CMLS*, **55**(6-7): 839–856.

Lau ESW, Zhang ZW, Qin MM, et al. 2016. Knockout of zebrafish ovarian aromatase gene (*cyp19a1a*) by TALEN and CRISPR/Cas9 leads to all-male offspring due to failed ovarian differentiation. *Scientific Reports*, **6**: 37357.

Li JZ, Ge W. 2020. Zebrafish as a model for studying ovarian development: Recent advances from targeted gene knockout studies. *Molecular and Cellular Endocrinology*, **507**: 110778.

Li MH, Sun YL, Zhao JE, et al. 2015. A tandem duplicate of anti-Müllerian hormone with a missense SNP on the Y chromosome is essential for male sex determination in Nile tilapia. *Oreochromis niloticus*. *PLoS Genetics*, **11**(11): e1005678.

Li N, Oakes JA, Storbeck KH, et al. 2020. The P450 side-chain cleavage enzyme Cyp11a2 facilitates steroidogenesis in zebrafish. *Journal of Endocrinology*, **244**(2): 309–321.

Li XY, Mei J, Ge CT, et al. 2022. Sex determination mechanisms and sex control approaches in aquaculture animals. *Science China Life Sciences*, **65**(6): 1091–1122.

Li Y, Li XH, Ye D, et al. 2024. Endogenous biosynthesis of docosahexaenoic acid (DHA) regulates fish oocyte maturation by promoting pregnenolone production. *Zoological Research*, **45**(1): 176–188.

Lin QH, Mei J, Li Z, et al. 2017. Distinct and cooperative roles of *amh* and *dmrt1* in self-renewal and differentiation of male germ cells in zebrafish. *Genetics*, **207**(3): 1007–1022.

Liu YL, Kossack ME, Mcfaul ME, et al. 2022. Single-cell transcriptome reveals insights into the development and function of the zebrafish ovary. *eLife*, **11**: e76014.

Love MI, Huber W, Anders S. 2014. Moderated estimation of fold change and dispersion for RNA-seq data with DESeq2. *Genome Biology*, **15**(12): 550.

Luzio A, Santos D, Monteiro SM, et al. 2021. Zebrafish male differentiation: Do all testes go through a "juvenile ovary" stage?. *Tissue and Cell*, **72**: 101545.

Matsuda M, Nagahama Y, Shinomiya A, et al. 2002. *DMY* is a Y-specific DM-domain gene required for male development in the medaka fish. *Nature*, **417**(6888): 559–563.

Nagahama Y, Chakraborty T, Paul-Prasanth B, et al. 2021. Sex determination, gonadal sex differentiation, and plasticity in vertebrate species. *Physiological Reviews*, **101**(3): 1237–1308.

Nanda I, Kondo M, Hornung U, et al. 2002. A duplicated copy of *DMRT1* in the sex-determining region of the Y chromosome of the medaka. *Oryzias latipes. Proceedings of the National Academy of Sciences of the United States of America*, **99**(18): 11778–11783.

Nishimura T, Sato T, Yamamoto Y, et al. 2015. *foxl3* is a germ cell-intrinsic factor involved in sperm-egg fate decision in medaka. *Science*, **349**(6245): 328–331.

Pan YJ, Tong SK, Hsu CW, et al. 2022. Zebrafish establish female germ cell identity by advancing cell proliferation and meiosis. *Frontiers in Cell and Developmental Biology*, **10**: 866267.

Qin MM, Xie QP, Wu K, et al. 2022. Loss of Nobox prevents ovarian differentiation from juvenile ovaries in zebrafish. *Biology of Reproduction*, **106**(6): 1254–1266.

Qin MM, Zhang ZW, Song WY, et al. 2018. Roles of Figla/*figla* in juvenile ovary development and follicle formation during zebrafish gonadogenesis. *Endocrinology*, **159**(11): 3699–3722.

Ribas L, Valdivieso A, Díaz N, et al. 2017. Appropriate rearing density in domesticated zebrafish to avoid masculinization: links with the stress response. *Journal of Experimental Biology*, **220**(Pt 6): 1056–1064.

Rodríguez-Marí A, Cañestro C, BreMiller RA, et al. 2013. Retinoic acid metabolic genes, meiosis, and gonadal sex differentiation in zebrafish. *PLoS One*, **8**(9): e73951.

Santos D, Luzio A, Coimbra AM. 2017. Zebrafish sex differentiation and gonad development: A review on the impact of environmental factors. *Aquatic Toxicology*, **191**: 141–163.

Schindelin J, Arganda-Carreras I, Frise E, et al. 2012. Fiji: an open-source platform for biological-image analysis. *Nature Methods*, **9**: 676–682.

Siegfried KR, Nüsslein-Volhard C. 2008. Germ line control of female sex determination in zebrafish. *Developmental Biology*, **324**(2): 277–287.

Slanchev K, Stebler J, De La Cueva-Méndez G, et al. 2005. Development without germ cells: the role of the germ line in zebrafish sex differentiation. *Proceedings of the National Academy of Sciences of the United States of America*, **102**(11): 4074–4079.

Tzung KW, Goto R, Saju JM, et al. 2015. Early depletion of primordial germ cells in zebrafish promotes testis formation. *Stem Cell Reports*, **4**(1): 61–73.

Uchida D, Yamashita M, Kitano T, et al. 2002. Oocyte apoptosis during the transition from ovary-like tissue to testes during sex differentiation of juvenile zebrafish. *Journal of Experimental Biology*, **205**(Pt 6): 711–718.

Wang XG, Bartfai R, Sleptsova-Freidrich I, et al. 2007. The timing and extent of 'juvenile ovary' phase are highly variable during zebrafish testis differentiation. *Journal of Fish Biology*, **70**(sa): 33–44.

Wang XS, Zhu JW, Wang HP, et al. 2023. Induced formation of primordial germ cells from zebrafish blastomeres by germplasm factors. *Nature Communications*, **14**(1): 7918.

Wang YQ, Ye D, Zhang FH, et al. 2022. *Cyp11a2* is essential for oocyte development and spermatogonial stem cell differentiation in zebrafish. *Endocrinology*, **163**(2): bqab258.

Webster KA, Schach U, Ordaz A, et al. 2017. Dmrt1 is necessary for male sexual development in zebrafish. *Developmental Biology*, **422**(1): 33–46.

Wilson CA, Batzel P, Postlethwait JH. 2024. Direct male development in chromosomally ZZ zebrafish. *Frontiers in Cell and Developmental Biology*, **12**: 1362228.

Wilson CA, High SK, McCluskey BM, et al. 2014. Wild sex in zebrafish: loss of the natural sex determinant in domesticated strains. *Genetics*, **198**(3): 1291–1308.

Wu K, Zhai Y, Qin MM, et al. 2023. Genetic evidence for differential functions of *figla* and *nobox* in zebrafish ovarian differentiation and folliculogenesis. *Communications Biology*, **6**(1): 1185.

Wu TZ, Hu EQ, Xu SB, et al. 2021. clusterProfiler 4.0: A universal enrichment tool for interpreting omics data. *The Innovation*, **2**(3): 100141.

Xu SS, Li Y, Wang HP, et al. 2023. Depletion of *stearoyl-CoA desaturase* (*scd*) leads to fatty liver disease and defective mating behavior in zebrafish. *Zoological Research*, **44**(1): 63–77.

Yang YJ, Wang Y, Li Z, et al. 2017. Sequential, divergent, and cooperative requirements of *Foxl2a* and *Foxl2b* in ovary development and maintenance of zebrafish. *Genetics*, **205**(4): 1551–1572.

Ye D, Liu T, Li YM, et al. 2023. Identification of fish spermatogenic cells through high-throughput immunofluorescence against testis with an antibody set. *Frontiers in Endocrinology*, **14**: 1044318.

Ye D, Zhu L, Zhang QF, et al. 2019. Abundance of early embryonic primordial germ cells promotes zebrafish female differentiation as revealed by lifetime labeling of germline. *Marine Biotechnology*, **21**(2): 217–228.

Zeng CW, Sheu JC, Tsai HJ. 2020. A new member of the forkhead box protein family in zebrafish: Domain composition, phylogenetic implication and embryonic expression pattern. *Gene Expression Patterns*, **35**: 119093.

Zhai G, Shu TT, Xia YG, et al. 2018. Characterization of sexual trait development in *cyp17a1*-deficient zebrafish. *Endocrinology*, **159**(10): 3549–3562.

Zhai Y, Zhang X, Zhao C, et al. 2023. Rescue of *bmp15* deficiency in zebrafish by mutation of *inha* reveals mechanisms of BMP15 regulation of folliculogenesis. *PLoS Genetics*, **19**(9): e1010954.

Zhang FH, Hao YK, Li XM, et al. 2022. Surrogate production of genome-edited sperm from a different subfamily by spermatogonial stem cell transplantation. *Science China Life Sciences*, **65**(5): 969–987.

Zhang FH, Li XM, He MD, et al. 2020a. Efficient generation of zebrafish maternal-zygotic mutants through transplantation of ectopically induced and Cas9/gRNA targeted primordial germ cells. *Journal of Genetics and Genomics*, **47**(1): 37–47.

Zhang QF, Ye D, Wang HP, et al. 2020b. Zebrafish *cyp11c1* knockout reveals the roles of 11-ketotestosterone and cortisol in sexual development and reproduction. *Endocrinology*, **161**(6): bqaa048.

Zhu B, Ge W. 2018. Genome editing in fishes and their applications. *General and Comparative Endocrinology*, **257**: 3–12.